

# The Clivus

## Anatomy, Normal Variants and Imaging Pathology

E. Hofmann · A. Prescher

Received: 27 March 2011 / Accepted: 23 May 2011 / Published online: 28 June 2011  
© Springer-Verlag 2011

**Abstract** The clivus is one of the most central parts of the skull base. As diseases of the clivus evade clinical evaluation imaging plays a pivotal role in establishing a diagnosis. This article combines the description of anatomy and pathology with an extensive pictorial essay. Starting with the development and normal macroscopic anatomy of the clivus the reader is then introduced to a large variety of normal variations and developmental disorders some of them with clinical significance. Typical examples of non-neoplastic and neoplastic masses of the clivus and their differential diagnoses are provided. The article concludes with a review of inflammatory disease and trauma.

**Keywords** Clivus · Skull base · Sphenoid bone · Computed tomography · Magnetic resonance imaging

### Introduction

The clivus (*Blumenbachii*) forms the central part of the base of the skull and is therefore an important structure. This osseous region is of great clinical importance because typical pathology, such as chordomas, metastatic tumors, inflammation and fibrous dysplasia, can occur there. The clivus is also involved in fractures and ultimately anatomical variations present important differential diagnostic issues.

The key to explaining these anatomical variations is having knowledge of their developmental history.

### Development of the Clivus

During early development the axial sclerotomes of the first somites are integrated into the skull base (Fig. 1) and form the basioccipital part [1]. Different opinions exist as to the number of axial sclerotomes incorporated into the skull base but it is now accepted that it consists of four elements [2, 3]. Because vertebral material is incorporated into the skull base the notochord or chorda dorsalis is an important developmental structure. It terminates just below the dorsum sellae and therefore the border between the spinal part and the chordal part of the skull base lies in front of the sphenoccipital fissure. The notochord describes a complicated course. First, it develops from the vertebral anlage, runs to the dorsal side of the primitive skull base and then perforates it in an oblique direction. It then emerges rostrally from the skull base to lie at the ventral (outer) side of the future clivus where irregular processes are formed. The notochord then enters the basisphenoid and ends directly under the dorsum sellae. In considering this topographical development it must be stated that the crista transversa of the adult skull does not mark the anterior end of the notochord but marks the location of the former sphenoccipital fissure.

Other important embryological structures that relate to the skull base are the hypochordal blastemas lying in front of the future vertebral bodies. Only the hypochordal blastema of the atlas is important as the anterior arch of the atlas is formed from this blastema. It is important that in regular development the hypochordal blastema of the proatlans is absorbed as well as that of the other vertebral levels. In cases of total or partial persistence of the hypochordal

---

E. Hofmann (✉)  
Klinik für Diagnostische und Interventionelle Neuroradiologie,  
Klinikum Fulda, Pacelliallee 4, 36043 Fulda, Deutschland  
e-mail: ehofmann.raz@klinikum-fulda.de

A. Prescher  
Institut für Anatomie, Medizinische Fakultät, RWTH Aachen,  
Aachen, Deutschland

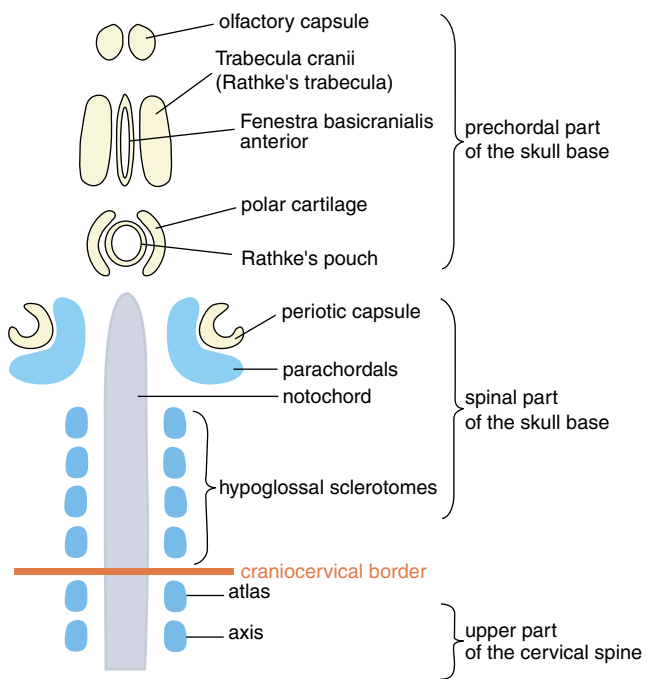


**Fig. 1** Schematic drawing of the early development of the skull base. Notice the four hypoglossal sclerotomes which are incorporated into the skull base forming the spinal part. The last incorporated hypoglossal sclerotome is designated as the proatlas

blastema of the proatlas, typical osseous variations at the caudal end of the clivus are formed [4]. If the central part persists, whereas the lateral parts diminish in size, a third condyle appears. If the lateral parts persist, whereas the central part diminishes, the basilar processes become evident. If the whole hypochordal blastema of the proatlas persists, the rare prebasiooccipital arch is manifest. Within the basilar part of the occipital bone the ossification center occurs between 11 and 12 weeks of fetal life [5]. As a rule only one ossification center is present but in rare cases it is possible that two centers, an anterior (basiotic sive prebasiooccipital) and

a posterior (basiooccipital), occur. The prechordal anlage of the basiooccipital part is expressed bilaterally. The rare segmentations of the clivus (transverse segmentation and sagittal clefts) can be explained according to these embryological conditions [6].

The clivus topographically ends at the sphenoccipital fissure just behind the dorsum sellae (Fig. 2a). This fissure must be regarded as an important central growth zone where the longitudinal growth of the skull base takes place. Ossification of this important zone takes place at an age of about 13–18 years (average 16 years) in boys and of about 12–16 years (average 14 years) in girls [7]. The sphenoccipital fissure or synchondrosis or cleft should not be mistaken for a fracture (Fig. 2b).

Physiological synostosis regularly starts at the upper parts of the sphenoccipital cleft. Only in some cases does an enchondral ossification center occur within the sphenoccipital cartilage. The anterior aspect of the basilar part of the occipital bone presents a typical morphology (Fig. 2c) and is D-shaped with the straight edge on the intracranial surface [5]. After closure of the sphenoccipital fissure the sphenoid bone and the occipital bone cannot be separated so that a new osseous unit is present. This central unit of the skull base should be termed as os tribasilare according to Rudolf Virchow [8].

According to this rudimentary discussion of development two points are important in explaining anatomical variations, malformations and pathological conditions:

1. If too much vertebral material is incorporated into the skull base, assimilation of the atlas occurs. If too little material is incorporated or if persistence of hypochordal material of the proatlas occurs, an occipital vertebra will be manifest. Manifestation of an occipital vertebra, a term introduced by Kollmann in 1905 [9], occurs in the region of the clivus in terms of the basilar processes, the third condyle and the prebasiooccipital arch. Moreover,



**Fig. 2** Fetal stage of the different components of the clivus (a). 1 Basilar part of the os occipitale, 2 os sphenoidale with its basisphenoidal part, 3 sphenoccipital synchondrosis, 4 anterior intraoccipital synchondroses. Note the small pits which are a characteristic feature of the

endocranial surface of the foetal clivus. Sphenoccipital synchondrosis (arrow) in the CT of a child (b). Anterior aspect of the pars basilaris ossis occipitalis (c). Notice the straight endocranial edge (arrow) and the irregular anterior surface presenting clefts and holes

different isolated ossicles may be present at the anterior margin of the foramen magnum [10].

2. The material of the chorda diminishes in size during further development. In some cases islands of chordoid material can persist within the clivus and begin to proliferate in later years. These proliferations were described by Virchow [8] as *ecchondrosis physaliphora* and constitute the matrix for typical tumors of the clivus, the chordomas. The term *ecchordosis physaliphora* is used nowadays for these non-neoplastic relations of clivus chordomas.

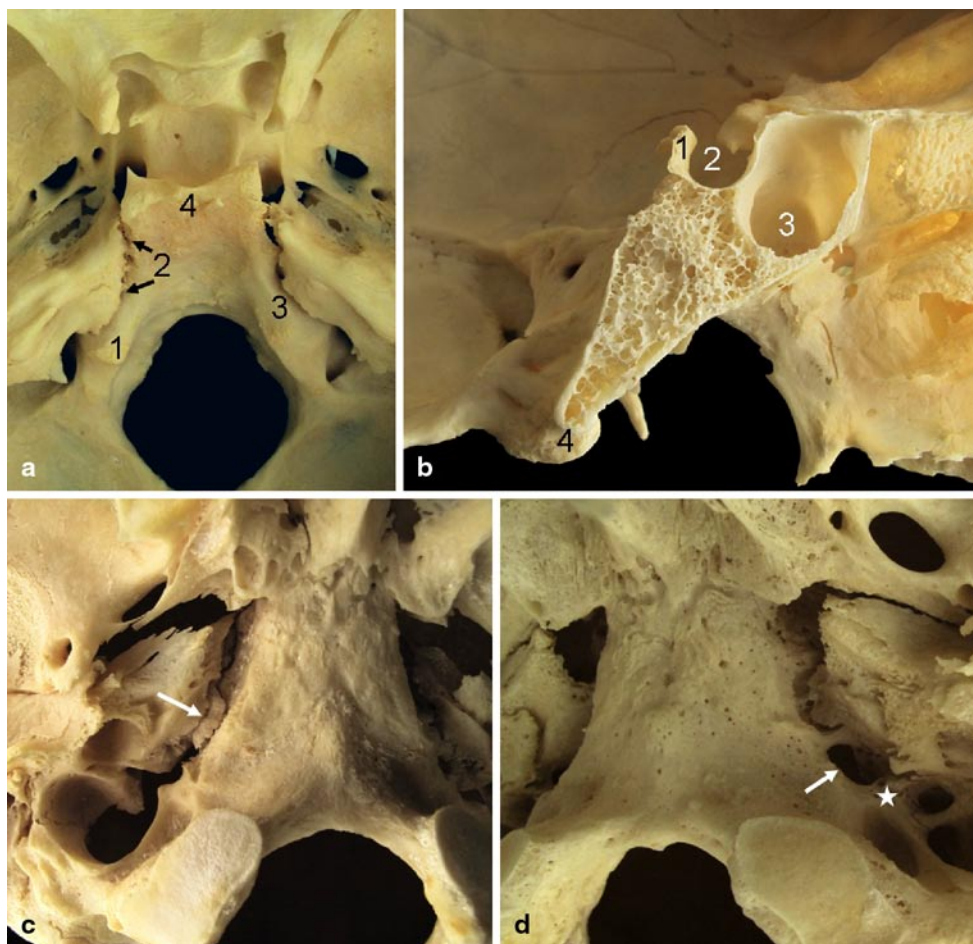
## Anatomy

### Cranial View

The osseous slope of the clivus (*Blumenbachii*) can be seen behind the *dorsum sellae* as it forms the anterior margin of the occipital foramen (Fig. 3a). The midsagittal section of the clivus (Fig. 3b) clearly presents a wedge-shaped appearance with a thin posterior and thick anterior part. A spongy structure can be easily identified which contains bone mar-

row. The clivus is separated laterally from the petrous part of the temporal bone by the petrooccipital fissure (*sive* petrobasilar fissure). This fissure is filled with cartilaginous tissue in adolescence so that a petrooccipital synchondrosis is formed in the nonmacerated skull. This synchondrosis ossifies during aging and in some cases small ossicles may be intercalated. These ossicles (Fig. 3c) are termed as *Riolan's ossicles* or *ossa raphogeminantes ossis petrosi*. According to Gruber [11], who described these ossicles in detail, these bones must be seen as sutural bones and not as epiphyses. There are many different forms, locations and entities of these ossicles, which explains the confusion in the literature. The *ossa raphogeminantes* are visible from the endocranium or the outside and in some cases they are hidden in the depth of the fissure. In some cases an additional foramen (Fig. 3d) may be present in the petrooccipital fissure which usually contains the inferior petrous sinus. This foramen is known as the *foramen pro sinu petroso inf. sive foramen anomalum suturae petro-basilaris* Gruber and can be seen in about 12% of cases. Cranially, the inferior petrous sinus rests on the petrooccipital fissure and creates the *sulcus sinus petrosi inferioris*. The clivus is not a plane but a dorsally concave structure. This concave depression is termed “*Clivusdelle*”

**Fig. 3** Clivus in the view from above (a). 1 *Tuberculum jugulare*, 2 *fissura petrooccipitalis*, 3 *sulcus sinus petrosi inferioris*, 4 *dorsum sellae*. Midsagittal section of the clivus (b). Note the typical wedge-shaped aspect of the clivus and the coarse spongiosa. 1 *Dorsum sellae*, 2 *sella turcica*, 3 *sinus sphenoidalis*, 4 *condylus occipitalis*. *Os raphogeminans ossis petrosi* (arrow c). This ossicle is intercalated into the *fissura petrooccipitalis* such that it is not able to fall out. Left-sided *foramen suturae petrobasilaris anomalum* Gruber (d white arrow) which is separated by an osseous bridge (asterisk) from the jugular foramen



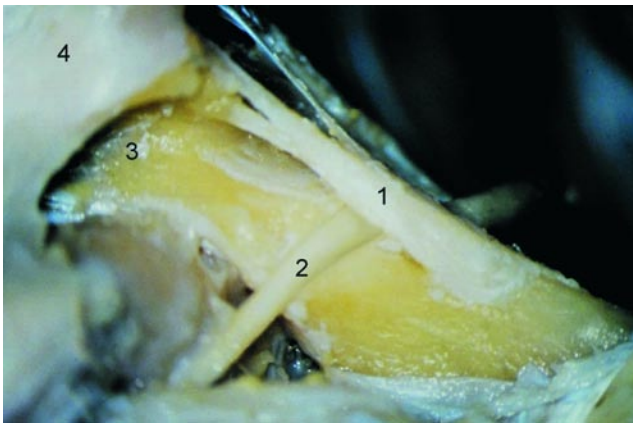


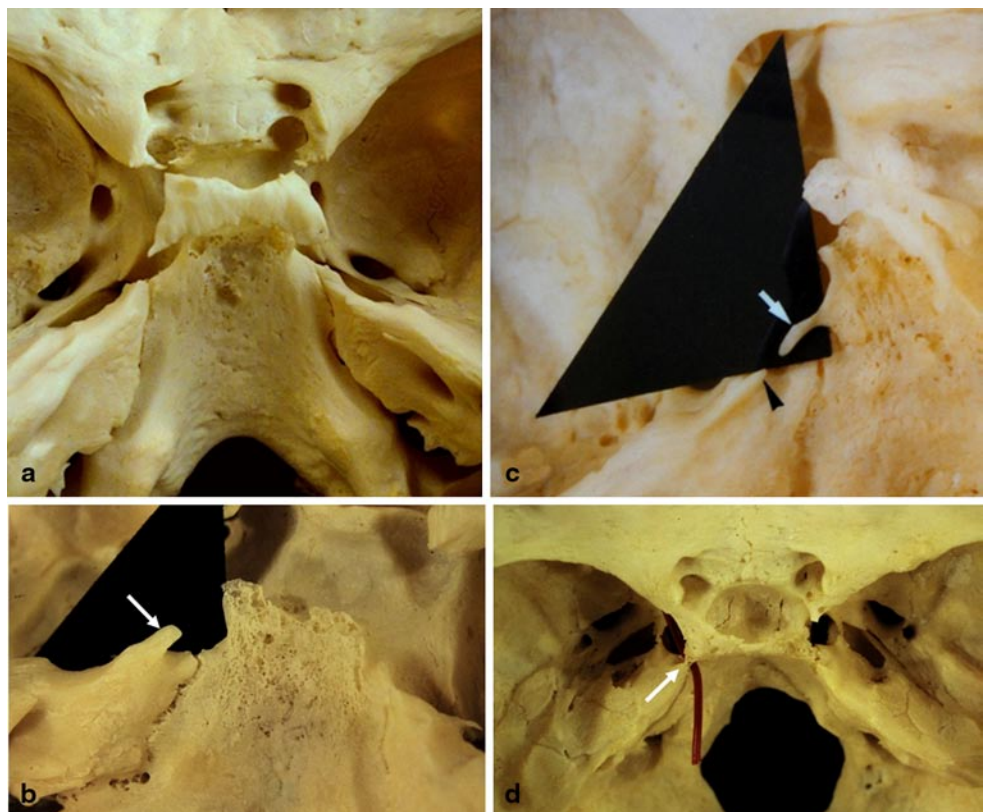
**Fig. 4** Abducens nerve lying under the superior sphenopetrosal ligament. 1 Lig. sphenopetrosum superius (Gruber), 2 nervus abducens, 3 apex partis petrosae, 4 dorsum sellae

(clivus dent) by Lang [12] or sulcus medullae oblongatae by von Spee [13].

The cranial surface is covered by dura mater which is perforated by the abducens nerves in the central part of the clivus. The abducens nerve then runs extradurally to the lateral margin of the dorsum sellae where it passes over the petrous apex and enters the cavernous sinus. At this point mention should be made of Dorello's canal with an explanation. Of several ligaments traversing the gap between the petrous apex and the lateral margin of the dorsum sellae,

the ligamentum petrosphenoideum (sive sphenopetrosum) superius, investigated with great precision by Gruber in 1859 [14], is important for the course of the abducens nerve. Microdissections of this region reveal the easily prepared petrosphenoidal or Gruber's ligament lying below the dura mater (Fig. 4). The ligament originates at the superior border of the pyramid and inserts at the posterior inferior clinoid process (sive processus petrosus posterior) and at the lateral margin of the dorsum sellae. It often splits into two or more bundles, some fading into the dura mater which covers the dural surface of the dorsum sellae. Several osseous situations may be observed depending on the degree of ossification of this ligament. The normal situation presents no ossification within the ligament at all (Fig. 5a), the ligament may be partially ossified at the superior crest of the petrous pyramid forming a processus sphenoidalis posterior (Fig. 5b) or ossification of the insertion at the lateral margin of the dorsum sellae produces a processus clinoides posterior inferior (Fig. 5c). It is rare to see complete ossification so that an additional osseous foramen occurs (Fig. 5d). This foramen should be termed foramen sphenopetrosum osseum anomalum Gruber. In contrast, the cross-sectional anatomy at microdissection (Fig. 6) of this region presents a more complicated situation: the abducens nerve is enclosed within a thin sheath of the cerebral dural layer and the trabeculated cavernous sinus extends around the abducens nerve. This venous space was termed the petroclival confluence

**Fig. 5** Normal situation at the petrous apex (a). Processus sphenoidalis posterior (b, arrow) at the superior margin of the petrous pyramid. Processus clinoides posterior inferior (c, white arrow). Small processus sphenoidalis posterior (black arrowhead). Foramen sphenopetrosum osseum anomalum (Gruber) cannulated with a red probe (d). The arrow points towards the osseous bridge



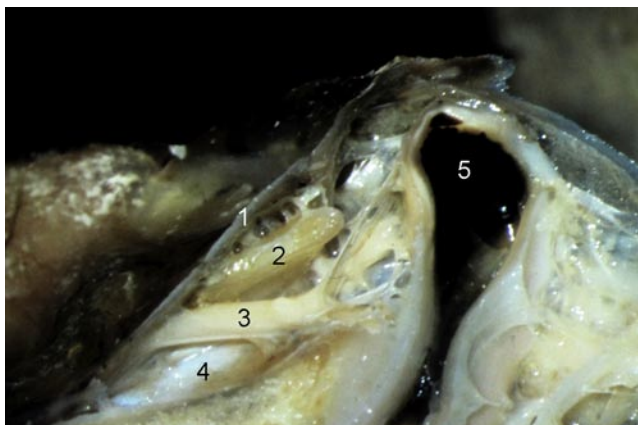


**Fig. 6** Section through the region of the petrous apex. 1 Dura mater, 2 lig. sphenopetrosum superius Gruber, 3 nervus abducens, 4 sinus petrosus inferior, 5 arteria carotis interna

by Destrieux et al. [15]. The inferior petrous sinus begins directly below the abducens nerve so that the nerve lies as a roof above the orifice of this sinus.

The abducens nerve passes through the foramen sphenopetrosum (fibrosum or osseum) and is fixed with its dural sheath at the superior margin of the petrous pyramid. The nerve may be compressed or stretched in this narrow passage especially during traumatic events. In the literature this conduit for the abducens nerve is also known as Dorello's canal but it should be noted that the concept of Dorello's canal, which is not a real canal, is no longer convincing as has already been described in the literature [15, 16]. On high-resolution magnetic resonance imaging (MRI) the abducens nerve can be followed from its cisternal portion up to the point where it crosses under Gruber's ligament (Fig. 7; [17]). A histologically proven arachnoid envelope around the petroclival segment of the nerve is shown as cerebrospinal fluid (CSF) evagination into Dorello's canal [18] on T2-weighted images.

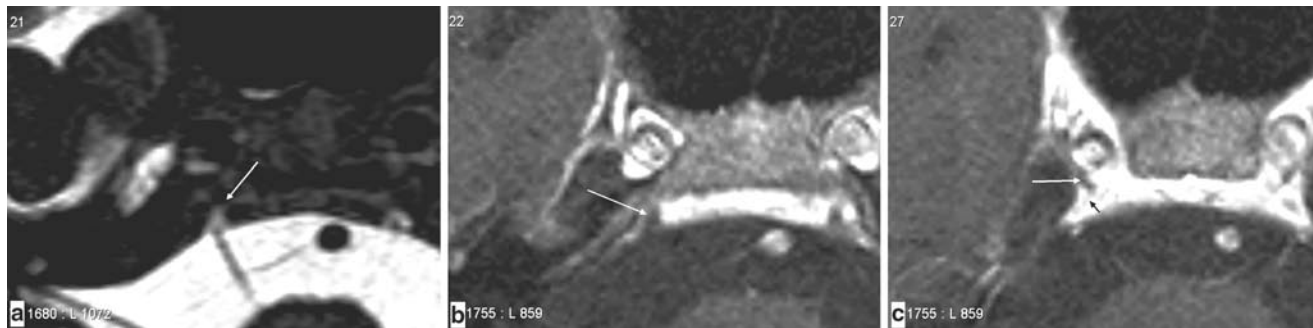


**Fig. 7** T2-weighted magnetic resonance imaging (a) at the level of entrance of the abducens nerve into "Dorello's canal" depicts evagination of cerebrospinal fluid. T1-weighted magnetic resonance imaging after contrast (b, c) shows the course of the abducens nerve (white arrow)

The sphenoid sinus if well pneumatized extends to the clivus with a posterior recess. In rare cases the sphenoid sinus can pneumatize the whole clivus and terminate at the anterior margin of the occipital foramen. It is essential for the ear, nose and throat (ENT) surgeon to recognize that the dorsal (superior) lamella of such a posterior recess of the sphenoid sinus is usually very thin or even dehiscent (Fig. 8) so that iatrogenic perforation can easily occur. A perforation of this thin lamella would be very dangerous for the basilar artery or the brain stem lying directly above the clivus.

#### Caudal View

If the clivus is considered from the caudal aspect it can be seen that it lies at the center of the skull base (Fig. 9) and at the anterior it is bordered by the vomer with its alae. Laterally it is separated from the petrous part of the temporal bone by the petrooccipital fissure in the posterior section and from the petrous apex by the foramen lacerum in the anterior part. Dorsally it forms the anterior margin of the foramen occipitale magnum. The anterior part of the clivus is smaller than the posterior one which merges with the lateral parts of the occipital bone. The outer surface of the clivus is covered in thick fibrous tissue which is a continuation of the fibrocartilago basalis of the foramen lacerum. It presents a complicated and variable relief [13, 19]. The terminology for the description of these osseous surface structures is not clearly defined and is often neglected in anatomy textbooks. The normally small pharyngeal tubercle is visible at a distance of about 1 cm from the anterior margin of the foramen magnum. This tubercle is the osseous fixing point for the raphe pharyngis and the anterior longitudinal ligament of the vertebral column. Therefore, topographically it marks the posterior extension of the pharyngeal roof. In some cases a small osseous elevation is present between the pharyngeal tubercle and the anterior margin of the foramen magnum. This ridge is called the crista pharyn-

through the venous plexus of the clivus with the abducens nerve (white arrow) crossing under Gruber's ligament (black arrow). All magnetic resonance images in this article were obtained from 1.5T scanners at the first author's institution



**Fig. 8** Posterior recess of the sphenoid sinus. The very thin, partially dehiscent structure of the superior wall is easily recognized. *Arrow:* dehiscence

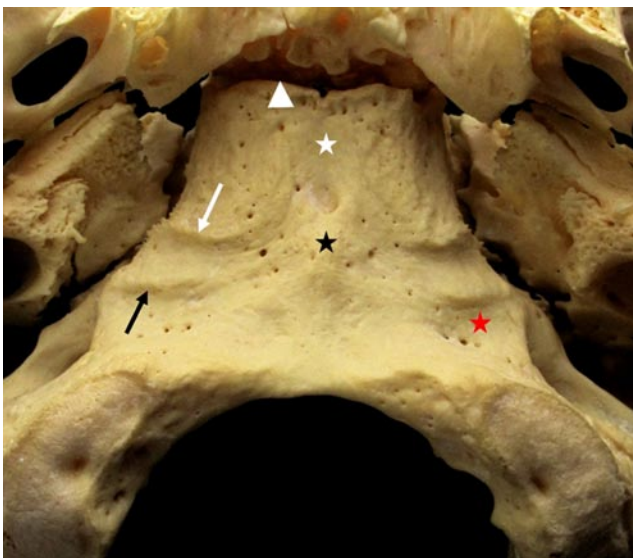


**Fig. 9** Caudal view of the clivus with the typical osseous relief. *Black asterisk* tuberculum pharyngeum, *white asterisk* fossa navicularis, *red asterisk* sulcus praecondylicus, *black arrow* crista muscularis, *white arrow* crista synostotica (Mingazzini), *white arrowhead* fissura sphenooccipitalis

gea. The osseous surface is characterized by two osseous ridges laterally to the pharyngeal tubercle. The anterior one is called the crista synostotica (Mingazzini), whereas the posterior one is termed the crista muscularis. Mingazzini's crista marks the border between the basioccipital and the prebasioccipital parts whereas the crista muscularis is due to the insertion of the rectus capitis anterior muscle. Often the crista muscularis borders the variable precondylar fossa (sive sulcus praecondylicus according to Jeschke [20]). A slight round or elliptical depression, the navicular fossa, may be observed in front of the pharyngeal tubercle.

#### Craniometry

As the basiocciput or the basilar part of the occipital bone is part of the clivus, the clivus is integrated in the craniocervical junction which comprises the occiput, atlas and axis [21]. With regard to basic craniometry the reader is referred to the relevant textbooks and review articles [21, 22]. Of the many lines and angles described, at least two should be remembered: the McRae line and the Boogaard angle. The McRae line or basion-opisthion line extends from the anterior margin of the foramen magnum (basion) to its posterior margin (opisthion). The odontoid tip commonly lies below this line. The Boogaard angle is described by the clivus plane (dorsum sellae to basion) and the McRae line. This angle should fall between  $119^\circ$  and  $135^\circ$  (mean  $122^\circ$ ; Fig. 10). Most anomalies are associated with a reduced angle and a decreased skull base height.

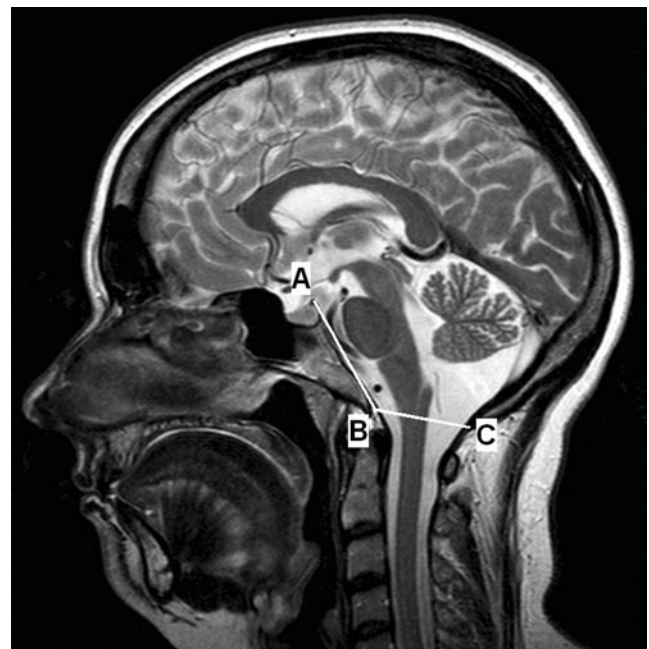


**Fig. 10** Basic craniometry of the clivus (T2-weighted midsagittal magnetic resonance image) showing the McRae line (BC) and the Boogaard angle (ABC)

## Anatomical Variations

### Basilar Transverse Fissure (Sausser's Fissure)

The extraordinarily rare basilar transverse fissure is a unilaterally or bilaterally incomplete or complete cleft or groove in the pars basilaris ossis occipitalis at the level of the pharyngeal tubercle (Fig. 11). This trait can be seen occasionally on x-rays of the paranasal sinuses [23]. Depending on the development of the basilar part of the occipital bone the basilar fissure marks the border between the basioticum and the basioccipital bone. For the various types of segmentation of the basioccipital bone see Le Double [6]. Confusion with the synchondrosis sphenoccipitalis which is normal in children and adolescents should be avoided. Radiologically, Sausser's fissure was first described in a case of atlas assimilation by List [24].

### Processus Basilares

Basilar processes are small bony bumps located at the anterior margin of the foramen magnum (Fig. 12). These excrescences may occur unilaterally or bilaterally, be firmly attached or form accessory ossicles [10, 25–27] and can be observed in approximately 4% of individuals [28]. Etiologically the basilar processes are derived from the hypochordal blastema of the proatlas which persists in its lateral parts. If excessive basilar processes fuse in the midline they could be confused with a third condyle. The osseous mass resulting from the fusion of the basilar processes is usually perforated by an osseous canal termed the canalis intrabasilaris Kollmanni. This canal does not exist in third condyles. The basilar processes do not seem to have any clinical significance besides differential diagnostic aspects. The articulation of a large basilar process with the anterior arch of the atlas is



**Fig. 11** Sausser's fissure in an incomplete form (arrows). Asterisk tuberculum pharyngeum, arrowhead crista pharyngea

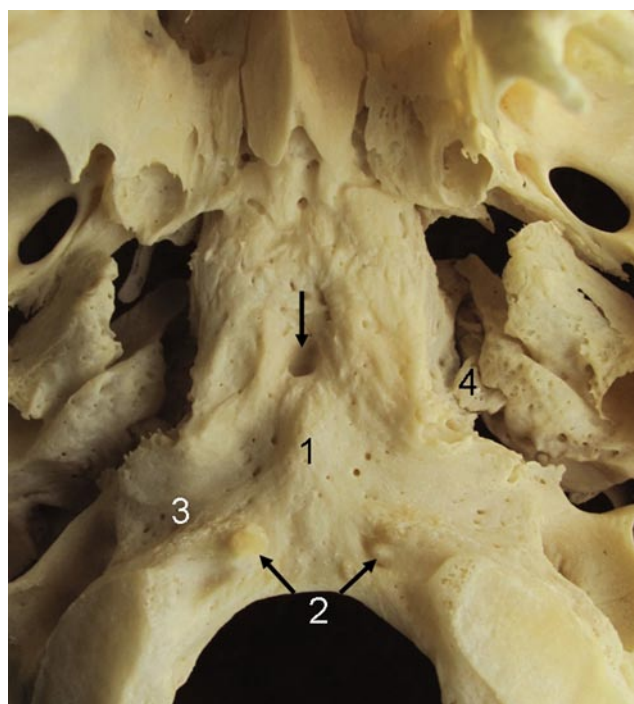


**Fig. 12** Clivus seen from below. 1 Tuberculum pharyngeum, 2 minimally expressed basilar processes, 3 sulcus praecondylicus, 4 small os raphogeminans ossis petrosi. Note additional pharyngeal foveola (arrow)

a rare event (Fig. 13a, b) and may lead to a serious disturbance of the mechanics of the atlantooccipital joint.

### Condylus Tertius

The condylus tertius (third condyle, Fig. 14a) results from persistence of hypochordal blastema of the proatlas in its medial part while the lateral parts diminish in size. The typical third condyle is an osseous process positioned in the mediosagittal plane at the anterior margin of the foramen magnum [10, 25–27] and was first described by Johann Friedrich Meckel jr. in 1815 [29]. In some cases an articulation occurs with the tip of the dens axis or the anterior arch of the atlas [25, 30, 31]. The third condyle may be of clinical significance because it may cause serious disturbances in skull mobility [22]. In rare cases a third condyle may be misinterpreted clinically as a nasopharyngeal tumor [32].

### Arcus Praebasioccipitalis

A horseshoe-like osseous mass at the anterior margin of the foramen occipitale magnum is referred to as prebasioccipital arch (Fig. 14b). This manifestation of the occipital vertebra may occur as isolated ossicles or a fixed element. The radiological appearance was studied in detail by one of us [26, 27]. The first typical radiological observation was published by Lombardi [33], who calculated a frequency

**Fig. 13** Large left-sided basilar process (**a**, *arrow*) showing the articular facet at the anterior arch of the atlas (*asterisk*) and the large basilar process articulating with the anterior arch of the atlas (**b**). The basilar process fits exactly into the fovea dentis

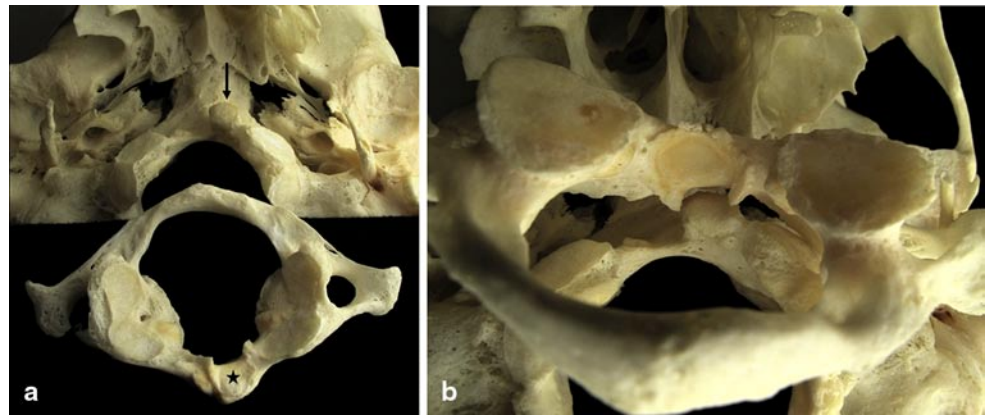
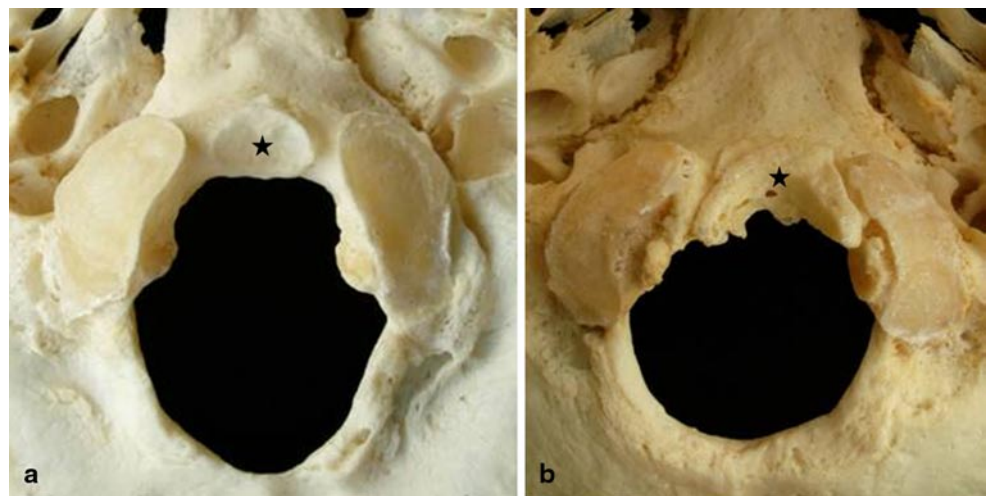


**Fig. 14** Condylus tertius (**a**, *asterisk*) with an articulation facet for the dens axis. Arcus praebasioccipitalis (**b**, *asterisk*) presenting as a horseshoe-like osseous mass at the anterior margin of the foramen occipitale magnum



of about 0.03%. The prebasioccipital arch can disturb the mechanics of the craniovertebral joints and the isolated element in particular may be dislocated into the spinal canal, due to traumatic events.

#### Ossification of the Ligamentum Apicis Dentis

The ligamentum apicis dentis (apical ligament of the odontoid process) is a developmental relic which can be derived from the notochord. This ligament has no mechanical properties, arises from the tip of the dens axis and inserts at the midsagittal point of the anterior margin of the foramen occipitale magnum. In some cases ossification can occur at the osseous fixing points. At the clivus the ossification mostly looks like a small osseous spur (Fig. 15a) and in rare cases only the ensheathing material ossifies, whereas the central part remains ligamentous. In such cases a tube-like structure occurs at the anterior margin of the foramen occipitale magnum (Fig. 15b). These ossifications of the ligamentum apicis dentis are of no clinical relevance but may in some cases be important for differential diagnostics and should

not be confused with the third condyle or the pseudocondylus tertius.

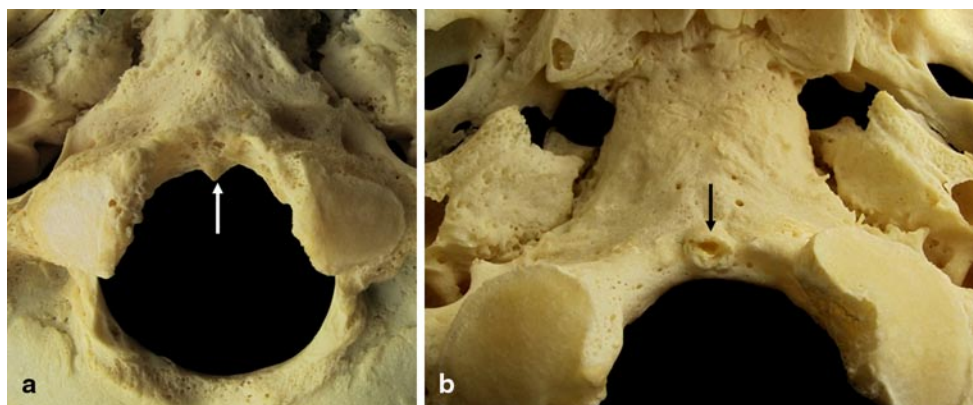
#### Nearthroses at the Clivus

During aging arthrotic changes frequently occur at the median atlantoaxial joint. This osteoarthrosis leads to osteophytes at the superior margin of the anterior arch of the atlas as well as at the anterior margin of the dens axis. In some cases these osteophytes come into contact with the medial part of the clivus where a typical nearthrosis is formed. These acquired conditions are to be differentiated from congenital entities which can also be modified by osteoarthrotic processes [25, 31, 34, 35].

#### Vessels

The clivus is covered by a venous plexus system which is in direct communication with the external and internal

**Fig. 15** Osseous spur (**a**, *arrow*) in the midsagittal plane of the anterior margin of the foramen occipitale magnum. This spur develops as an ossification of the ligamentum apicis dentis. Small tubular osseous structure (**b**, *arrow*), also due to an ossification of the ligamentum apicis dentis



vertebral venous plexuses. Because developmentally the clivus belongs to the vertebral column, the basilar venous plexuses can be seen as a part of Batson’s plexus. According to these venous connections the clivus is often reached by metastatic tumors affecting the vertebral column. Breast carcinomas and prostatic cancer in particular often involve the clivus.

**Developmental Disorders**

The basiocciput which contributes to the lower part of the clivus is formed by four occipital sclerotomes. Nonfusion of these sclerotomes allows for a variety of gaps that can be seen by imaging. Bony canals, if present, are assumed to contain communicating veins between extracranial and intracranial venous plexuses [36] and such passages are a regular finding on high-resolution computed tomography (CT) (Fig. 16) but the prevalence and significance are barely known.



**Fig. 16** Transclival venous canal (*white arrows*) on sagittal computed tomography. Incidental finding in a patient with an invasive pituitary adenoma (*arrow*: erosion of sellar floor)

**Basilar Canals**

In some cases a canalis basilaris (Fig. 17) may be present in the basal part of the occipital bone. Usually this canal contains a vein or venous plexus which can be seen as former basivertebral veins of the vertebral material which was incorporated into the skull base. The vein within the basilar canal forms an anastomosis between the intracranial and extracranial venous systems. A frequency of 8% in adults may be calculated for the canalis basilaris [37]. Different subgroups have been described and are summarized by Lang [12]. If a pharyngeal foveola is present the basilar canal may open into this osseous depression.

Of the subgroups a median basilar canal is a well-defined channel originating on the intracranial surface of the basiocciput in the midline close to the anterior rim of the foramen magnum (Fig. 18). Two theories have been proposed regarding the embryogenesis: one is vascular and the second and more likely theory implies vestiges of the notochordal canal [38]. A median basilar canal has a fairly high prevalence of 20% in the skulls of newborns and becomes increasingly



**Fig. 17** Basilar canal, cannulated with a red probe opening in front of the pharyngeal tubercle (*asterisk*)

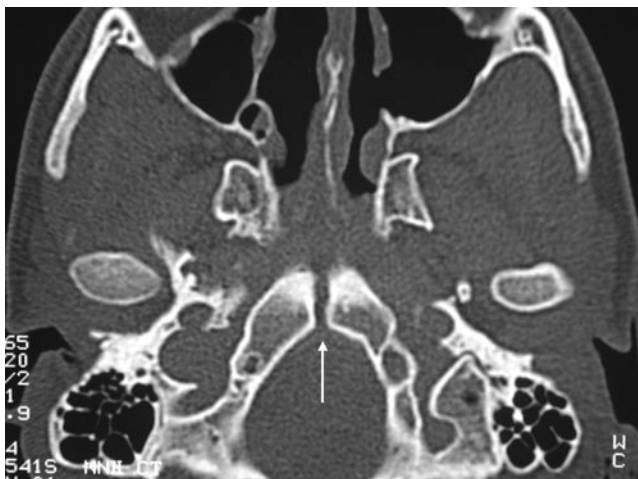


**Fig. 18** Axial CT of a median basilar canal (*arrow*) in a male teenager suffering from recurrent bacterial meningitis

rare in adult age where it is found in only 1% [39]. Contrary to previous assumptions of a basilar canal being a meaningless, innocent normal variation there is evidence that this anomaly may be a weak point in the skull base and has to be actively sought in patients with bacterial meningitis [40].

A median basilar canal may open in front of the pharyngeal tubercle at the level of the pharyngeal fossa or foveola on the inferior surface of the sphenoid.

#### Pharyngeal Fossa or Pharyngeal Foveola

A pharyngeal fossa or pharyngeal foveola may or may not be associated with a basilar canal and may be an isolated finding. It is a round or oval recess found occasionally in the base of an inconstant bony excavation, the fossa navicularis, located in the midline in front of the pharyngeal tuberosity at the inferior surface of the clivus [41, 42]. Only in rare cases is a typical pharyngeal foveola (sive pharyngeal fossa) present in this region presenting as a blind

ending hole or funnel (see Fig. 11). The pharyngeal foveola was first described by Tourtual [43] and Pölchen [44] also investigated this blind ending hole and correlated it with the pharyngeal bursa. It is interesting that this bursa may extend into the foveola in cases of Tornwaldt's cysts. Gruber [45] differentiated three different types of the pharyngeal foveola, the foveola pharyngea infundibuliformis posterior, foveola infundibuliformis media vera and foveola pharyngea infundibuliformis anterior. A pharyngeal foveola may have clinical significance and apart from posing differential diagnostic problems for imaging it might play a role in enabling ascending meningitis (Fig. 19).

#### Arachnoid Herniations

Nontraumatic osseous defects of the clivus with arachnoid herniation can lead to spontaneous CSF leaks into the sphenoid sinus and ultimately to bacterial meningitis. Such defects are associated with intracranial hypertension and occur most frequently within the ethmoid and within the inferolateral recess of the sphenoid sinus, the midline sphenoid sinus ranking third in frequency [46]. In the clivus the defects penetrate the posterior wall of the sphenoid sinus allowing for small arachnoid pits to herniate into the sinus lumen (Fig. 20). Inexperience with this finding and their small size can cause such midsphenoid leaks to be easily overlooked.

#### Nonneoplastic Masses

##### Fibrous Dysplasia

Fibrous dysplasia is a developmental anomaly with the replacement of mature bone by structurally weak immature woven bone and fibrous tissue and is most often seen in the first decades of life. It occurs in two forms: polyostotic,

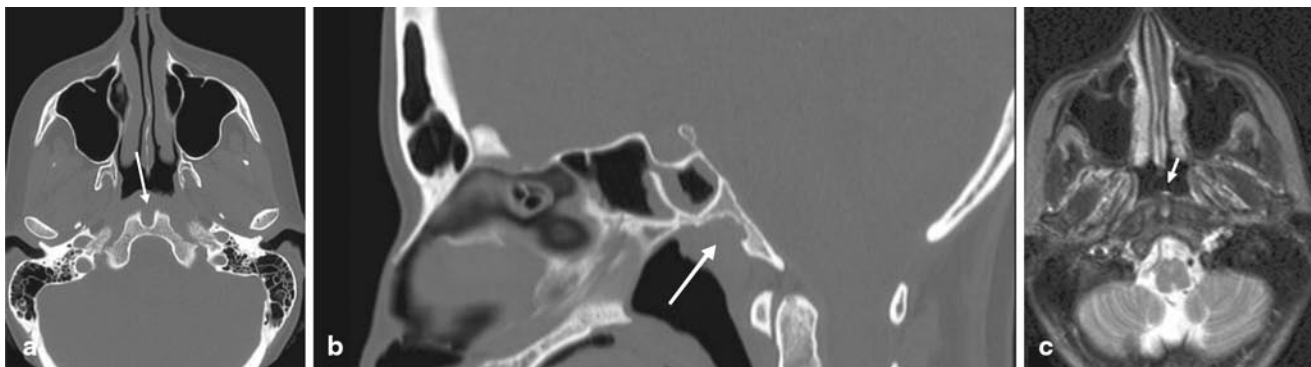


**Fig. 19** Pharyngeal foveola (*arrow*), axial (a) and sagittal (b) reformation of computed tomography in an 8-year-old girl with meningitis. No other entrance for an infectious agent could be found. Association

of pharyngeal foveola with a Tornwaldt cyst (c, *arrow*) on T2-weighted magnetic resonance imaging

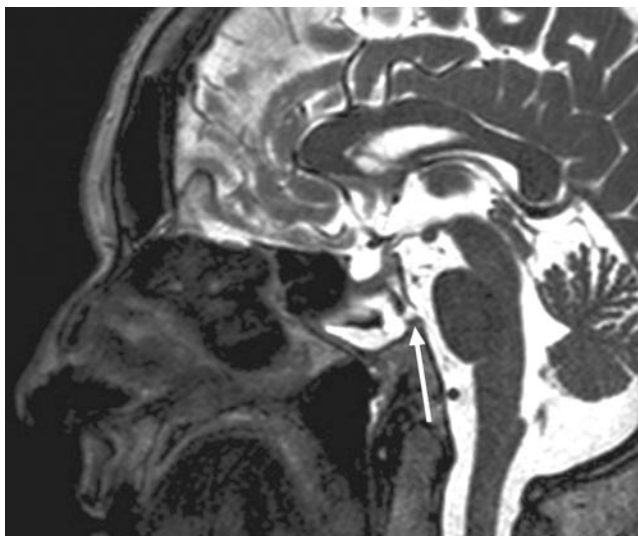


**Fig. 20** T2-weighted sagittal magnetic resonance imaging. Arachnoid hernia through a small defect in posterior sphenoid wall (*arrow*). Note associated empty sella

involving several bones and making up 30% of the cases and monostotic, which involves a single bone and constitutes 70% of cases [47]. Polyostotic fibrous dysplasia, in addition to café au lait spots and endocrine disorders, constitutes the McCune-Albright syndrome. Involvement of the sphenoid bone and clivus is not uncommon [48] in fibrous dysplasia of the skull base but involvement of the clivus in monostotic fibrous dysplasia is rare. Imaging findings are characteristic and CT shows thinning of cortical bone and expansion of the affected area with the typical ground-glass appearance (Fig. 21). Usually, the diagnosis is straightforward and should obviate the need for biopsy. The MRI findings are less specific and T1-weighted images invariably exhibit a low signal. The signal on T2-weighted images may vary from low in cellular, fibrous areas to high in areas of cyst formation.

#### Neurenteric Cysts

A neurenteric cyst of the clivus is an unusual cause for a clival mass [49]. On CT a lytic lesion with intact cortex should arouse suspicion of a neurenteric cyst, which is hyperintense (relative to gray matter) on T1-weighted and iso-intense to hypo-intense on T2-weighted MRI and is a differential diagnosis of sphenoid sinus mucocele.

#### Ecchordosis Physaliphora

A lesion which has only recently been described systematically is ecchordosis physaliphora [50], a tumor-like congenital malformation, formerly incorrectly designated as ecchondrosis physaliphora. It is anything but rare and can be found in 2% of autopsies and thin-section MR imaging stu-



**Fig. 21** Extensive fibrous dysplasia of the skull base involving the clivus

dies. Ecchordosis physaliphora consists of nodules of gelatinous tissue considered to be an ectopic notochord remnant. Imaging is characteristic: the lesion arises from the clivus at the midline from where it protrudes into the intradural prepontine cistern (Fig. 22) and a stalk-like median bony protuberance or crest is a diagnostic hallmark. Ecchordoses are hyperintense on T2-weighted MRI and hypointense on T1-weighted MRI. In contrast to their neoplastic kinship, chordomas, they do not show contrast enhancement [51]. Formerly considered to be a clinically inconspicuous incidental finding, ecchordosis physaliphora has recently been ascribed to bleeding or to causing CSF leakage [52, 53].

### Neoplastic Masses

#### Chordoma

Ecchordosis physaliphora and chordoma are closely related lesions which share a common histologic origin, namely that they are both remnants of the notochord. Chordomas in contrast to ecchordoses are slow growing, locally invasive malignant neoplasms which can metastasize via hematogenous or lymphatic routes. The rare purely intradural chordoma is difficult to distinguish from ecchordosis physaliphora and poses a differential diagnostic challenge in terms of histology and radiography.

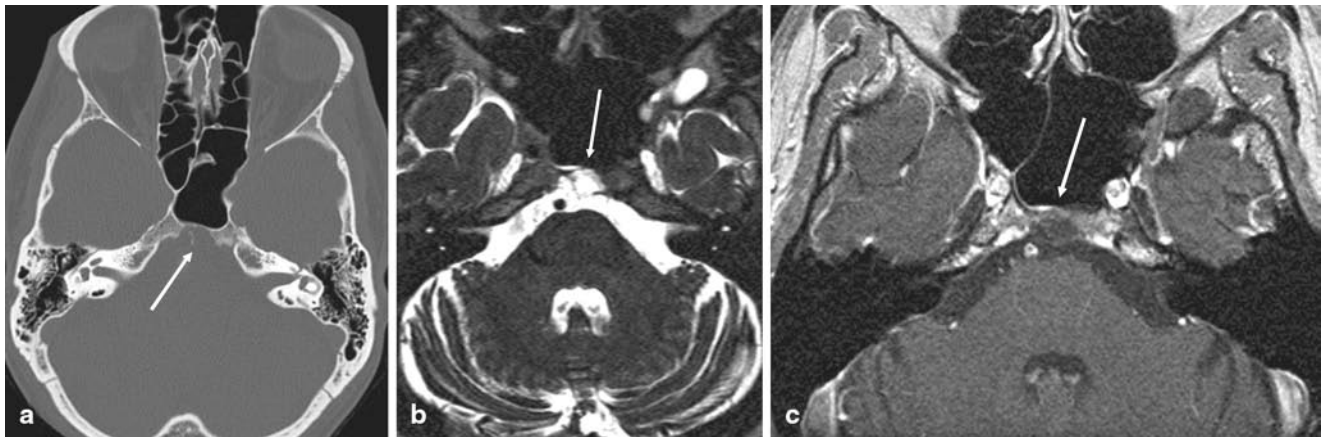


**Fig. 22** Echordosis physaliphora. Median crest-like bony stalk (**a**, arrow on axial computed tomography). Non-enhancing clival mass (**b** and **c**, arrow on T2-weighted and T1-weighted magnetic resonance imaging with contrast) in an asymptomatic male

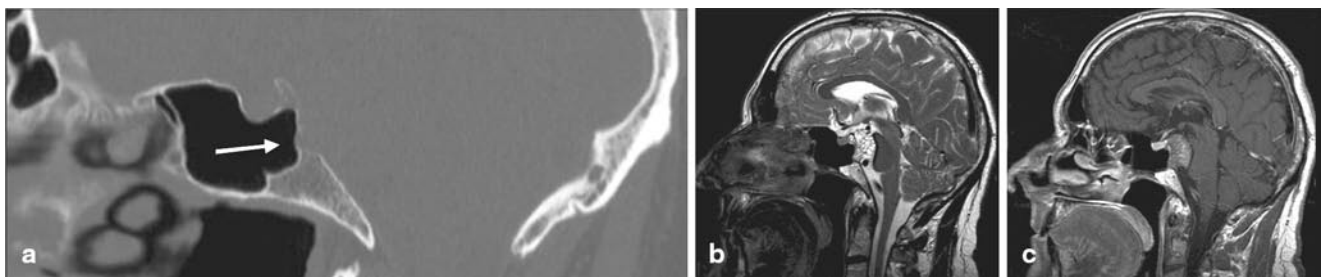


**Fig. 23** Clivus chordoma. Subtle bony erosion on computed tomography (**a** arrow). Extensive tissue tumor in the prepontine cistern (**b** magnetic resonance imaging T2-weighted, **c** T1-weighted with contrast) with encroachment of the basilar artery

Classical clival chordomas account for 1% of intracranial tumors [54] and due to their slow growth are insidious in producing symptoms (headache, diplopia). They typically appear as centrally located, well-circumscribed, expansile soft-tissue masses which most often arise from the clivus with associated lytic bone destruction. A minority of chordomas arise unilaterally from the petrous apex. On CT clival chordomas appear as lytic bone destruction with an associated expansile soft-tissue mass. Intratumoral calcium deposits are irregular and are thought to be sequestra from bone destruction. Chordomas appear bright on T2-weighted MRI, a finding which reflects their high fluid content, while on T1-weighted MRI they are dark and show moderate to marked contrast enhancement which may be heterogeneous (Fig. 23). Foci of hemorrhages appear as bright spots on T1-weighted and dark areas on gradient-weighted sequences. Metastases, lymphatic or hematogenous, should always be sought.

### Meningioma

The clivus is covered with dura mater, therefore it can be affected by the most common tumor of the dura, meningioma. Originating from arachnoidal granulations at the

vicinity of the petroclival line, meningiomas are very rare at the center of the clivus proper (Fig. 24). This may be due to a relative paucity of arachnoid granulations at the central surface of the clivus. Petroclival meningiomas (Fig. 25) are

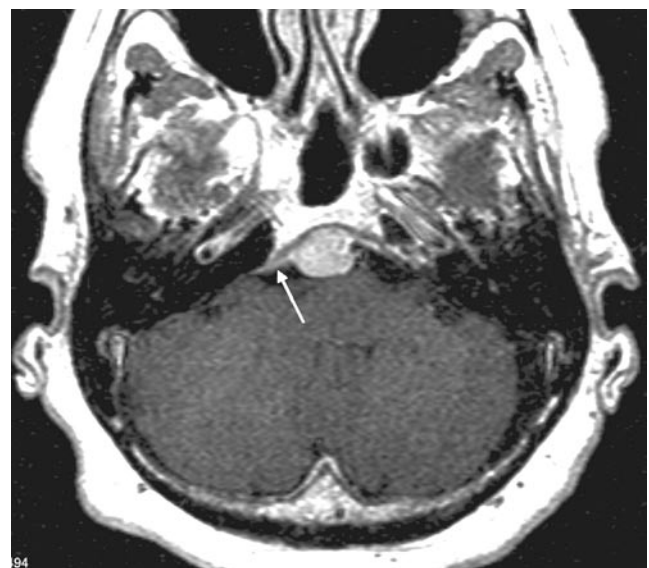
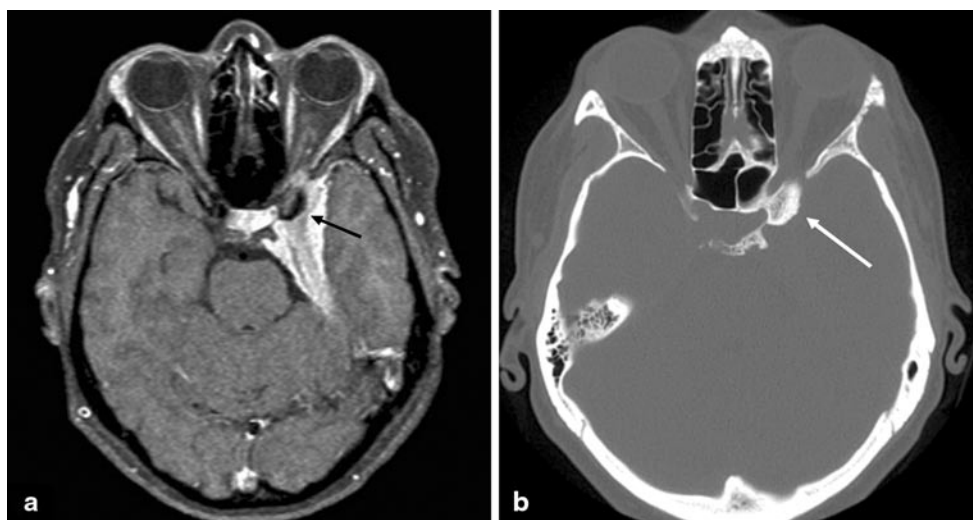


**Fig. 24** Central meningioma of the clivus with typical dural tail (T1-weighted magnetic resonance imaging with contrast, arrow)

**Fig. 25** Petroclival meningioma with two-sided infiltration of the tentorial margin and petroclival fold. Note sclerotic anterior clinoid process (*arrow*). T1-weighted magnetic resonance imaging with contrast (**a**) and axial computed tomography (**b**)



much more common and are defined as being located medial to the exit of the trigeminal nerve [55]. Usually, the tentorium is invaded whereby one-sided invasion is limited to the posterior fossa, while two-sided invasion also affects the middle fossa through the tentorial incisura [56]. While some clival meningiomas are entirely dural and subdural others may have a tendency to involve the extradural and osseous compartments [57]. Special care should be undertaken to analyze vascular encasement and displacement especially of the carotid artery.

#### Metastasis

Like any region of the skull the clivus can be affected by bone metastases. Depending on the primary tumor, metastases may appear as focal or confluent areas of osteolysis or osteosclerosis. While being considered as rare findings in a neurosurgical patient sample [58] it is the authors' expe-

rience that clival metastases are not uncommon. The most common primaries are breast and prostate cancer (Fig. 26). The communicating venous network of the clivus and the spine facilitates the spread of tumor cells. In osteolytic lesions, plasmocytoma is a differential diagnosis (Fig. 27).

#### Tumors of Adjacent Compartments

A description of clival tumors is not complete until mention has been made of adjacent regions and their neoplasias. As a part of the sphenoidal and occipital bones the clivus is prone to be involved in a variety of tumors of neighboring structures. In the anterior, the dorsal extension of an invasive pituitary adenoma can reach the clivus. Laterally, trigeminal schwannomas may extend to the clivus leading to scalloping of its laterodorsal surface. On rare occasions, even tumors arising from the jugular foramen or cerebello-pontine cistern can extend as far as the clivus.

**Fig. 26** Osteoplastic clival metastasis of prostate carcinoma with extension into suprasellar cistern with computed tomography (**a**) and T2-weighted magnetic resonance imaging (**b**). Note signal void on magnetic resonance imaging which is difficult to distinguish from air in the sphenoid sinus

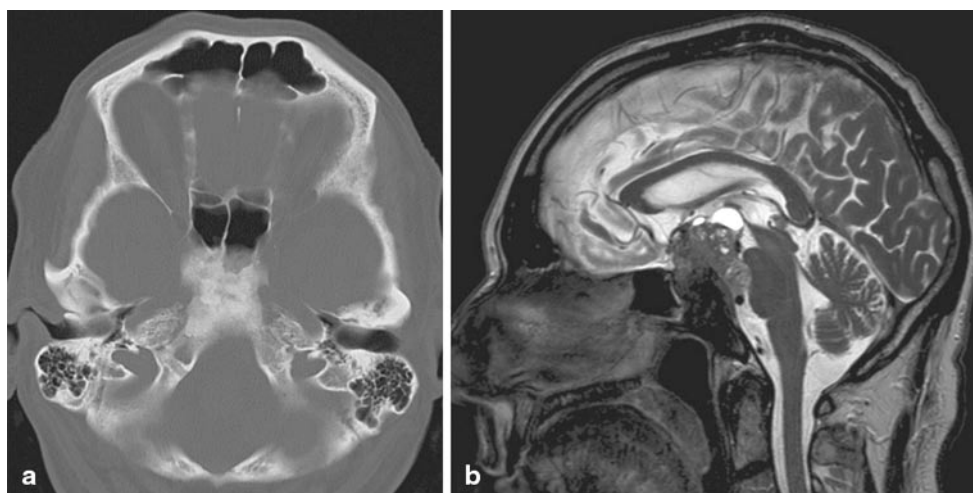


**Fig. 27** Clival plasmocytoma (arrows) on axial computed tomography (a) and T1-weighted magnetic resonance imaging with contrast (b)



## Inflammatory Lesions

### Chronic Sinusitis

Pneumatization of the sphenoid sinus may vary considerably [59]. In the so-called post-sellar type the sphenoid sinus reaches the clivus in the posterior with its mucoperiosteum coming into close contact with the dura mater of the prepontine cistern. In this situation the clivus is prone to be affected by sphenoid sinusitis. In chronic infections of the sphenoid sinus its walls are thickened and sclerotic and the cavity shrunken [60]. This gives the clivus a sclerotic appearance (Fig. 28).

### Skull Base Osteomyelitis

Skull base osteomyelitis mimics malignancy. It may follow external ear infection in older diabetic or otherwise immunocompromised patients, mostly males and has *Pseudo-*



**Fig. 28** Sagittal CT. Chronic sphenoid sinusitis with marked sclerosis of posterior sphenoid sinus wall

*monas aeruginosa* as the usual pathogen. Patients usually present with ear pain and otorrhea. Associated cranial nerve neuropathy, mostly double vision, facial palsy, facial pain and hoarseness, indicates skull base involvement [61]. Atypical skull base osteomyelitis arises from the sphenoid or occipital bones, is not associated with external otitis, occurs far less frequently and initially may have headache as the only symptom [62]. Skull base osteomyelitis is potentially life-threatening and requires urgent diagnosis and treatment. Imaging is one of the mainstays in establishing the diagnosis and CT findings are cortical bone erosion and adjacent soft tissue swelling [63]. The MRI findings are replacement of clival fatty bone marrow by exudate and effacement of soft tissues resulting in a marked drop of T1-weighted signal in precontrast images (Fig. 29). The soft tissues and bones involved are greatly enhanced after iv contrast medium.

### Inflammatory Pseudotumor

Very rarely, inflammatory pseudotumors may involve the clivus and mimic malignancy. A soft tissue mass lesion, with extension into the prevertebral retropharyngeal space and the cavernous sinuses, is detected by CT and MRI [64].

## Traumatic Lesions

Fractures of the clivus are not uncommon and have been reported in 0.2% of patients with head injuries and in 2% of patients with skull fractures [65]. Historically associated with a disastrous prognosis, the outcome with a mortality of about 25% is better than has been described before the advent of high-resolution CT. Clival fractures can be classified as three types: (1) sagittal (intersecting the dorsum sel-

**Fig. 29** Skull base osteomyelitis. Slight cortical erosions on computed tomography (*arrows in a*) and extensive soft tissue involvement on T1-weighted magnetic resonance imaging (*arrows in b*)

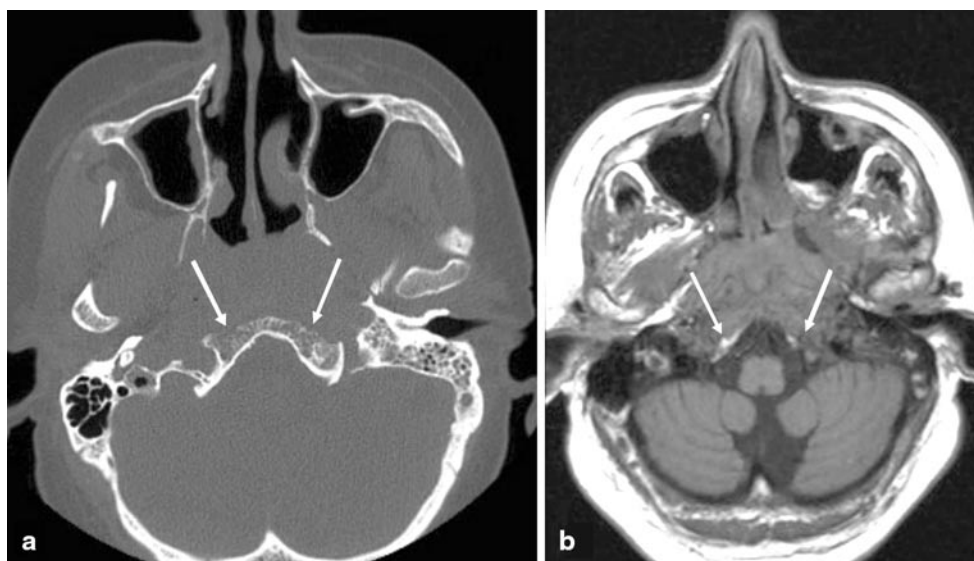


**Fig. 30** Clival fractures. Sagittal type (*arrows in a*), transverse type (*arrows in b*) and oblique type (*arrows in c*)

lae), (2) transverse (intersecting both petrous ridges) and (3) oblique (intersecting one petrous ridge; Fig. 30). Oblique fractures are most common with longitudinal and transverse fractures ranking second and third, respectively. Those patients with a transverse fracture have the highest risk of death. The vertebrobasilar arteries can be trapped in rare cases of clivus fractures [66].

Traumatic retroclival hematomas are rare [67] and most reported cases have involved pediatric patients [68] where hematomas can be subdural or epidural. In contrast to reports in the literature the only patient encountered by the authors in recent years was an elderly man who developed a traumatic subdural retroclival hematoma following adequate trauma (Fig. 31). Clinicians should be highly suspicious of ligamentous injury and the potential instability of the craniocervical junction.

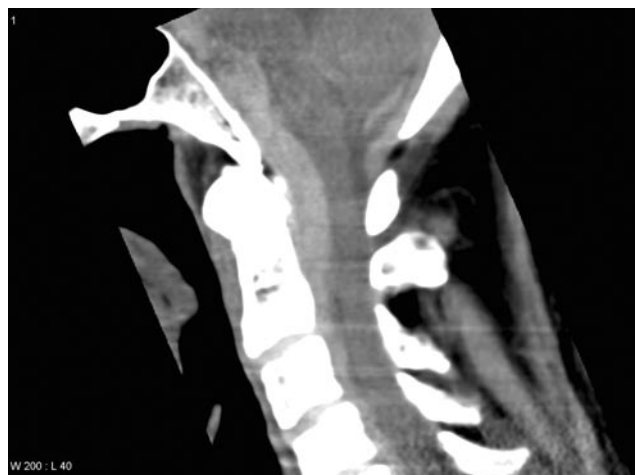


**Fig. 31** Sagittal CT. Extensive extra-axial hematoma extending from the retroclival area into the cervical spinal canal

## Conclusions

The clivus is the central part of the skull base. Often, clinical signs and symptoms of clival disease are nonspecific or even absent, therefore, imaging is one of the mainstays for establishing a diagnosis. This necessitates a thorough knowledge by the neuroradiologist of normal anatomy, the sometimes insidious normal variants and frank pathology.

**Acknowledgement** Dedicated to the first author's teacher and mentor, Prof. Dr. L. Solymosi in friendly relationship on the occasion of his 60th birthday.

**Conflict of Interest** The authors declare that there are no actual or potential conflicts of interest in relation to this article.

## References

- Christ B, Jacob HJ, Jacob M, Seifert R, Hinrichsen K. Über die Entwicklung der kranio-zervikalen Übergangsregion. *Verh Anat Ges.* 1987;81:565–6.
- Clara M. *Entwicklungsgeschichte des Menschen.* Leipzig: Thieme; 1966.
- O'Rahilly R, Müller F. The early development of the hypoglossal nerve and occipital somites in staged human embryos. *Am J Anat.* 1984;169:237–57.
- Putz R. Zur Manifestation der hypochordalen Spangen im cranio-vertebralen Grenzgebiet beim Menschen. *Anat Anz.* 1975;137:65–74.
- Scheuer L, Black S. *Developmental juvenile osteology.* San Diego: Academic Press; 2000.
- Le Double AF. *Traite des variations des os du crane de l'homme.* Paris: Vigot Freres; 1903.
- Melsen B. Time and mode of closure of the spheno-occipital synchondrosis determined on human autopsy material. *Acta Anat.* 1972;83:112–8.
- Virchow R. Untersuchungen über die Entwicklung des Schädelgrundes im gesunden und krankhaften Zustande und über den Einfluß derselben auf die Schädelform, Gesichtsbildung und Gehirnbau. Berlin: Reimer; 1857.
- Kollmann J. Varianten am Os occipitale, besonders in der Umgebung des Foramen occipitale magnum. *Anat Anz.* 1905;27(Suppl):231–6.
- Prescher A. The differential diagnosis of isolated ossicles in the region of the dens axis. *Gegenbaurs Morph Jahrb.* 1990;136:139–54.
- Gruber W. Beiträge zur Anatomie des Schädelgrundes. 1. Abtlg. *Memoires de L'Academie imperiale des sciences de St.-Petersbourg.* 1869; 7. Serie, Tome 8:1–34.
- Lang J. Teil B: Gehirn- und Augenschädel. Springer: Berlin; 1979.
- Graf von Spee F. *Skelettlehre, 2. Abt.: Kopf.* In: von Bardeleben K, editor. *Handbuch der Anatomie des Menschen.* Gustav Fischer: Jena; 1896.
- Gruber W. Beiträge zur Anatomie des Keilbeines und Schläfenbeines. *Imperatorskaja Akademija Nauk (St. Petersburg).* 1859; 7. Serie, Tome 1(3):3–14.
- Destrieux C, Velut S, Kakou MK, Lefrancq T, Arbeille B, Santini JJ. A new concept in Dorello's canal microanatomy: the petroclival venous confluence. *J Neurosurg.* 1997;87:67–72.
- Prescher A, Brors D, Schick B. Topographische Anatomie der Felsenbeinspitze und des Dorello-Kanals. In: Bootz F, Strauss G, editors. *Die Chirurgie der lateralen Schädelbasis.* Berlin: Springer; 2002. pp. 31–35.
- Yousri I, Camelio S, Wiesmann M, Schmid UD, Moriggl B, Brückmann H, et al. Detailed magnetic resonance imaging anatomy of the cisternal segment of the abducent nerve: Dorello's canal and neurovascular relationships and landmarks. *J Neurosurg.* 1999;91:276–83.
- Ono K, Arai H, Endo T, Tsunoda A, Sato K, Sakai T, et al. Detailed MR imaging anatomy of the abducent nerve: evagination of CSF into Dorello canal. *AJNR Am J Neuroradiol.* 2004;25:623–6.
- Rouviere H. *Anatomie humaine. Descriptive et topographique.* Vol. 10. Tome 1. Paris: Masson; 1967.
- Jeschke K. *Ueber den Sulcus praecondylicus des Hinterhauptbeins.* Diss. Königsberg; 1894.
- Smoker WR. Craniovertebral junction: normal anatomy, craniometry, and congenital anomalies. *Radiographics.* 1994;14:255–77.
- Von Torklus D, Gehle W. *Die obere Halswirbelsäule.* Stuttgart: Thieme; 1987. pp. 19–20.
- Köhler A, Zimmer EA. Grenzen des Normalen und Anfänge des Pathologischen im Röntgenbild des Skeletts. 13. neubearb. Aufl. Stuttgart: Thieme; 1989.
- List CF. Neurologic syndromes accompanying developmental anomalies of the occipital bone, atlas and axis. *Arch Neurol Psychiatry.* 1941;45:577–616.
- Prescher A. The craniocervical junction in man, the osseous variations, their significance and differential diagnosis. *Ann Anat.* 1997;179:1–19.
- Prescher A, Brors D, Adam G. Anatomic and radiologic appearance of several variants of the craniocervical junction. *Skull Base Surg.* 1996;6:83–94.
- Prescher A, Brors D, Adam G. Beitrag zur Kenntnis des anatomischen und radiologischen Erscheinungsbildes einiger ausgewählter Varianten des kraniozervikalen Überganges. In: Hausamen JE, Schmelzeisen R, editors. *Traumatologie der Schädelbasis.* Reinbek: Einhorn-Press; 1996.
- Misch M. Beiträge zur Kenntnis der Gelenkfortsätze des menschlichen Hinterhauptes und der Varietäten in ihrem Bereiche. Diss. Berlin; 1905.
- Meckel JF. Über einige Abnormitäten der Knochen. *Dtsch Arch Physiol (Halle/Berlin).* 1815;1:641–4.
- Von Lüdinghausen M, Fahr M, Prescher A, Schindler A, Kenn W, Weiglein A, et al. Accessory joints between basiocciput and atlas/axis in the median plane. *Clin Anat.* 2005;18:558–71.
- Von Lüdinghausen M, Prescher A, Kageya I, Yoshimura K. The median atlantooccipital joint in advanced age. *Spine* 2006;31: E430–6.
- Will CH. Condylus tertius, einen Nasenrachentumor vortäuschend. *RöFo.* 1980;133:557–8.
- Lombardi G. The occipital vertebra. *Am J Roentgenol.* 1961;86:260–9.
- Olsson O. Arthrosis deformans des vorderen Zahngelenks. *RöFo.* 1944;66:233–9.
- Prescher A, Brors D. Die Arthrosis deformans der Articulatio atlantooccipitalis mediana: morphologische Folgen für den kraniozervikalen Übergang und klinische Bedeutung. In: Lanksch WR, Lehmann N, Hrsg. *Die hintere Schädelgrube und der kraniozervikale Übergang.* Reinbek: Einhorn-Press; 1998. pp. 240–7.
- Chauhan NK, Chopra J, Rani A, Rani A, Srivastava AK. A bony canal in the basilar part of occipital bone. *Int J Anat Variat.* 2010;3:112–3.
- Oehmke HJ. Die Bedeutung des Canalis basilaris und seine Darstellung im Röntgenbild. *Gegenbaurs Morphol Jahrb.* 1963;104:459–75.

38. Jacquemin C, Bosley TM, Al Saleh M, Mullaney P. Canalis basilaris medianus: MRI. *Neuroradiology*. 2000;42:121–3.
39. Fiegler W. Der Canalis basilaris medianus im Röntgenbild und Computertomogramm. *RöFo*. 1980;133:416–9.
40. Schick B, Prescher A, Hofmann E, Steigerwald C, Draf W. Two occult skull base malformations causing recurrent meningitis in a child: a case report. *Eur Arch Otorhinolaryngol*. 2003;260:518–21.
41. Currarino G. Canalis basilaris medianus and related defects of the basiocciput. *Am J Neuroradiol*. 1988;9:208–11.
42. Fiegler W, Stolle E. Die Foveola pharyngea—Darstellung im konventionellen Tomogramm und in der Computertomographie. *RöFo*. 1980;133:188–91.
43. Tourtual C Th. Neue Untersuchungen über den Bau des menschlichen Schlund- und Kehlkopfes. Leipzig: Otto Wigand; 1846.
44. Pölchen R. Zur Anatomie des Nasenrachenraumes. *Arch Pathol Anat Physiol Klin Med*. 1890;119:118–26.
45. Gruber W. Ueber die bis jetzt unter der Firma der Norm angegebene, jedoch bestimmt anomale und in drei Arten auftretende Foveola pharyngea an der Pars basilaris des Os occipitale. In: *Beobachtungen aus der menschlichen und vergleichenden Anatomie*. IX. 1889;Heft:2–9.
46. Schuknecht B, Simmen D, Briner HR, Holzmann D. Nontraumatic skull base defects with spontaneous CSF rhinorrhea and arachnoid herniation: imaging findings and correlation with endoscopic sinus surgery in 27 patients. *Am J Neurorad*. 2008;29:542–9.
47. Atalar M, Ozum U. Monostotic fibrous dysplasia of the clivus: Imaging findings. *Turk Neurosurg*. 2010;20:77–81.
48. Lustig LR, Holliday MJ, McCarthy EF, Nager GT. Fibrous dysplasia involving the skull base and temporal bone. *Arch Otolaryngol Head Neck Surg*. 2001;127:1239–47.
49. Kapoor V, Johnson DR, Fukui MB, Rothfus WE, Iho HD. Neuroradiologic-pathologic correlation in a neurenteric cyst of the clivus. *Am J Neurorad*. 2002;23:476–9.
50. Mehnert F, Bechornr R, Küker W, Hahn U, Nägele T. Retroclival echordosis physaliphora: MR imaging and review of the literature. *Am J Neurorad*. 2004;25:1851–5.
51. Srinivasan A, Goyal M, Kingstone M. Case 133: echordosis physaliphora. *Radiology*. 2008;247:585–8.
52. Alli A, Clark N, Mansell NJ. Cerebrospinal fluid rhinorrhea secondary to echordosis physaliphora. *Skull Base*. 2008;18:395–9.
53. Alkan Ö, Yildirim T, Kizilkilic O, Tan M, Cekinmez M. A case of echordosis physaliphora presenting with an intratumoral hemorrhage. *Turk Neurosurg*. 2009;19:293–6.
54. Erdem E, Angtuaco EC, Van Hemert R, Park JS, Al-Mefty O. Comprehensive review of intracranial chordoma. *Radiographics*. 2009;23:995–1009.
55. Lobato RD, Gonzalez P, Alday R, Ramos A, Lagares A, Alen JF, Palomino JC, Miranda P, Perez-Nunez A, Arrese I. Meningiomas of the posterior fossa. Surgical experience in 80 cases. *Neurocirugia*. 2004;15:525–42.
56. Kawase T, Shiobara R, Ohira T, Toya S. Developmental patterns and characteristic symptoms of petroclival meningiomas. *Nurol Med Chir*. 1996;36:1–6.
57. Sekhar LN, Jannetta PJ, Burkhart LE, Janosky JE. Meningiomas involving the clivus: a six-year experience with 41 patients. *Neurosurgery*. 1990;27:764–81.
58. Pallini R, Sabatino G, Doglietto F, Lauretti L, Fernandez E, Maira G. Clivus metastases: report of seven patients and literature review. *Acta Neurochir (Wien)*. 2009;151:291–6.
59. Lang J. Clinical anatomy of the nose, nasal cavity and paranasal sinuses. Stuttgart: Thieme; 1989.
60. Som PM, Brandwein M. Sinonasal cavities: Inflammatory disorders, tumors, fractures and postoperative findings. In: Som PM, Curtin HD, editors. *Head and neck imaging*. Vol. 2. St. Louis: Mosby; 1996. p. 134.
61. Lee S, Hooper R, Fuller A, Turlakow A, Cousins V, Nouraei R. Otogenic cranial base osteomyelitis: a proposed prognosis-based system for disease classification. *Otol Neurotol*. 2008;29:666–72.
62. Chang PC, Fischbein NJ, Holliday RA. Central skull base osteomyelitis in patients without otitis externa: imaging findings. *Am J Neurorad*. 2003;24:1310–6.
63. Cavel O, Fliss DM, Segev Y, Zik D, Khafif A, Landsberg R. The role of the otolaryngologist in the management of central skull base osteomyelitis. *Am J Rhinol*. 2007;21:281–5.
64. Lee JH, Kim K, Chung SW, Choi YC, Lee A. A case report of inflammatory pseudotumor involving the clivus: CT and MRI findings. *Korean J Radiol*. 2001;2:231–4.
65. Ochalski PG, Spiro RM, Fabio A, Kassam AB, Okonkwo DO. Fractures of the clivus: a contemporary series in the computed tomographic era. *Neurosurgery*. 2009;56:1063–9.
66. Sato S, Iida H, Hirayama H, Endo M, Ohwada T, Fuji K. Traumatic basilar artery occlusion caused by a fracture of the clivus. *Neurol Med Chir*. 2001;41:541–4.
67. Guillaume D, Menezes AH. Retroclival hematoma in the pediatric population. *J Neurosurg (4 Suppl Pediatrics)*. 2006;105:321–25.
68. McDougall CM, Sankar T, Mehta V, Pugh JA. Pediatric traumatic retroclival epidural hematoma. *Can J Neurol Sci*. 2011;38:338–40.